International Journal of Rock Mechanics & Mining Sciences 76 (2015) 146–154

Contents lists available at ScienceDirect

International Journal of Rock Mechanics & Mining Sciences

journal homepage: www.elsevier.com/locate/ijrmms

Technical Note

Effects of strain rate on fracture characteristics and mesoscopic failure mechanisms of granite

Changyu Liang [a,b], Shuren Wu [a,b], Xiao Li [c], Peng Xin [a,b,*]

[a] Key Laboratory of Neotectonics Movement & Geohazards, Ministry of Land and Mineral Resource, Beijing 100081, PR China
[b] Institute of Geomechanics, Chinese Academy of Geological Sciences, Beijing 100081, PR China
[c] Key Laboratory of Engineering Geomechanics, Institute of Geology and Geophysics, Chinese Academy of Sciences, Beijing 100029, PR China

ARTICLE INFO

Article history:
Received 11 August 2014
Received in revised form
16 January 2015
Accepted 6 March 2015
Available online 27 March 2015

1. Introduction

A substantial effort has been made towards investigating the mechanical behavior of rock materials over a wide range of loading rates [1–15]. It is fundamental to make research on rock damage and failure properties under dynamic loading such as blasting, explosion and earthquake. It has been generally accepted that mechanical properties and the corresponding fracture process of brittle rock are rate-dependent under quasi-static loading [16–20]. However, the studies on the failure process and failure mechanism of brittle rocks under dynamic loading are inconclusive. This may result from insufficient data, perhaps due to the limitations of experimental apparatus and the complexity of rock microstructure. Additional tests are required to examine various possibilities, and to explore the essence of rock fracture and its rate-dependence.

The topography of rock fracture surfaces often reveals the inherent details of the deformation and fracture, while the energy characteristics of failure process governs the fracture surface topography [6,11,21–23]. Some previous studies were employed on the meso-morphology of fracture using the Scanning Electron Microscope (SEM), and to a certain extent the difference of failure mechanism between high and quasi-static loading rates is analyzed [11,24,25]. Furthermore, a substantial effort has been devoted to perform the quantitative analysis on the energy of rock failure process [6,11]. It has been interestingly found that the probable relations between the energy and meso-morphology characteristics can be established during the failure process, in which the more the energy is absorbed, the more the rock fragments are observed.

Although the results of fracture behaviors of brittle materials have been obtained by experimental observations, fractal geometry theory, theoretical analysis and numerical modeling, there have been very few studies on characterizing failure micromechanism over a wide range of strain rates [25]. Research on micromechanism is fundamental to have a deep insight of rock fracture. In this paper, attempts are made to explore the topic of fracture behaviors of rock by considering the fracture characteristics and failure mechanisms. Systematic experimental studies have been performed to study failure process, fracture characteristics and failure micromechanisms of rock at both low and intermediate strain rates in the range of 10^{-5}–$10^{-1}\,s^{-1}$ at the macroscopic and microscopic scales. The experimental procedures from which the characterizations of fracture process derived are described. A detailed description of experimental observations on the macroscopic scale is presented. The fractography at the mesoscopic level is examined.

2. Rock material

The rock material used in this study is a coarse-grained dark granite from Jinzhou, Liaoning province, China. Microscopic studies were performed to give an insight of the mineralogical composition and grain sizes, as shown in Fig. 1. As listed in Table 1, the main compositions are quartz (~40%) and feldspar (~55%).

The uniaxial compression tests were conducted using the ISRM suggested method [26]. The samples are prepared with the dimension (diameter × height) of 49.5 mm × 125.7 mm. The

* Corresponding author at: Key Laboratory of Neotectonics Movement & Geohazards, Ministry of Land and Mineral Resource, Beijing 100081, PR China. #Tel.: +86 10 88815109; fax: +86 10 68422326.
E-mail address: mechxinp@126.com (P. Xin).

http://dx.doi.org/10.1016/j.ijrmms.2015.03.010
1365-1609/

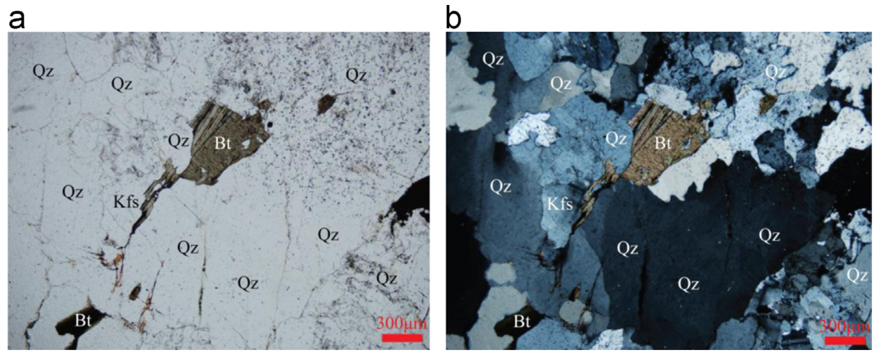

Fig. 1. Micrographs of the granite using an optical microscope.(a) Plane polarized light. (b) Cross polarized light.

Table 1
The main component of granite (%).

Quartz	Plagioclase	Alkali feldspar	Hornblend	Biotite	Iron object	Phosphorite	Zircorn
40	35	20	2	<3	<1	<1	<1

sample numbers were different for each group of strain rate according to the experimental conditions. At low strain rate, due to the long loading time, the growth and development of crack in each sample may be different, and the mechanical properties and fracture characteristics are different. It is thus necessary to choose more samples to represent properties under low strain rates. With the increase of strain rate, the crack development is inadequate, and the mechanical properties are basically the same, and therefore the numbers of samples can be less. As shown in Table 2, in the column of sample ID, S represents static tests, D represents dynamic tests, and SA, SB, DA, DB represent group A and group B of quasi-static tests and dynamic tests, respectively. The corresponding strain rates are 10^{-5}, 10^{-4}, 10^{-3} and 10^{-2} s^{-1}. If the test is unsuccessful, or the data obtained in the test is abnormal or the corresponding data is not collected because of the set of sampling interval, experimental data and the ID will not be listed in the table, such as the lack of SA-1-3.

3. Dynamic loading test system

A new dynamic loading system has been developed at the Institute of Geology and Geophysics, Chinese Academy of Science. It is a hydraulic servo-controlled machine with the frequency of 0.01–5 HZ and the strain rate $\acute{\varepsilon}$ can be achieved up to 10^{-1} s^{-1}. The high-stiffness steel main frame (with system stiffness of 5 GN/m) and axial actuator (with the maximum axial stress of 1000 kN), high-precision double close loop serve control design (with channel resolution of $\pm$ 100,000 levels) and electro-hydraulic servo response design (with the maximum work stress of 34.475 MPa and the frequency response of 70 Hz), high-precision dynamic measurement system and test operational software subsystem ensure the reliance of experimental data at the intermediate strain rates.

The system has two kinds of controlling modes according to the requirement of different strain rates, which are the deformation and the displacement controlling modes, respectively. When strain rate $\acute{\varepsilon}$ is less than 10^{-4} s^{-1}, the deformation control method is adopted; while $\acute{\varepsilon} > 10^{-4}$ s^{-1}, the displacement control method is used to achieve the target strain rate, which is a ratio of the strain to the duration time calculated after a test.

The axial and radial deformations are measured by the linear variable different transformer (LVDT) devices. The sampling interval depends on the strain rate: when the strain rate is low, sampling interval takes 0.02 s; and when $\acute{\varepsilon} > 10^{-3}$ s^{-1}, sampling interval is set to 1 ms. During the testing, a computer is applied to record the real-time stress and strain data.

Table 2
Stress threshold and the corresponding strain of granite under different strain rates.

ID	$\acute{\varepsilon}/s^{-1}$	σ_{ci} /MPa	ε_{ci}	σ_f /MPa	ε_f
SA-1-1	0.00001	85.1	0.00280	158.466	0.00469
SA-2	0.00001	105.0	0.00262	154.561	0.00408
SA-1-4	0.00001	67.3	0.00243	122.538	0.00414
SA-1-5	0.00001	49.3	0.00258	108.825	0.00471
SA-1-6	0.00001	80.1	0.00241	147.305	0.00402
SB-1	0.00010	83.2	0.00280	128.370	0.00436
SB-2	0.00010	87.2	0.00275	144.248	0.00445
DA-2	0.00154	102.0	0.00290	168.049	0.00470
DA-1-1	0.00163	90.4	0.00277	166.807	0.00456
DB-2	0.02110	102.0	0.002 88	188.644	0.00473
DB-1-1	0.02470	165.0	0.00358	222.078	0.004 68

4. Experimental results and discussions

4.1. Stress–strain curves

Fig. 2 shows the stress–strain curves of rock samples at various strain rates. It can be seen that with the increase of strain rate, the stress and strain increase, but the strain growth is not evident. Meanwhile, it is easy to find that the stress and strain of both SA and SB searies are very close, which properly means that when $\acute{\varepsilon} < 10^{-4}$ s^{-1}, the stress and the strain are not very sensitive to the strain rate. The conclusions are consistent with the authors' previous research results [27].

4.2. Progressive failure process of granite

Brace [16], Hallbauer et al. [18], Hoek [19] and Martin [20] performed tests on brittle rocks and found that the failure process could be categorized into the following five stages, namely crack closure stage I, linear elastic deformation stage II, crack initiation and crack stable growth stage III, crake damage and unstable crack growth IV, failure and post peak stage V. In fact, the progressive failure process of rock is the process of microcrack development in rock. The division of each stage depends on three important stress threshold values, which are crack initiation stress σ_{ci}, dilatancy